KLA

Strain Rate Sensitivity of Thin Metal Films by Instrumented Indentation

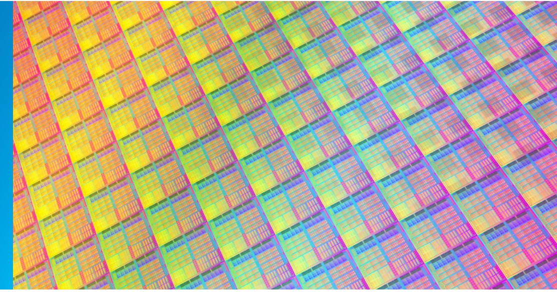

Introduction

Strain rate sensitivity (SRS) is an important material property because it quantifies the tendency of the material to creep. Materials that do not creep have a near-zero strain rate sensitivity. For materials with high strain rate sensitivity, small stresses can cause plastic deformation if the strain rate is sufficiently small. In this note, we present a new technique for measuring strain rate sensitivity by instrumented indentation that is insensitive to thermal drift and can be used for thin films and other small volumes.[1,2] We demonstrate the technique by using it to measure the strain rate sensitivity of thin copper and nickel films deposited on silicon, and we compare our results to those that have been published for comparable materials. Maier et al. measured the strain rate sensitivity of ultrafine-grained nickel by instrumented indentation to be 0.019, and they compared this value to the results of uniaxial testing on the same material which gave a value of 0.016.[3] Ye et al. consolidated strain rate sensitivity measurements that have been published for copper and presented them as a function of grain size.[4] For grain sizes on the order of 100nm–1500nm, reported values for strain rate sensitivity of copper varied between 0.005 and 0.02. These ranges (0.016–0.019 for nickel; 0.005–0.02 for copper) set our expectations for the present work.

Theory

In traditional (uniaxial) creep testing, the relationship between plastic stress, σ, and strain rate, $\dot{\varepsilon}_u^m$, is expressed as:

$$\sigma = B^* \dot{\varepsilon}_u^m \quad \text{Eq. 1}$$

where B* is a constant and m is the strain rate sensitivity (SRS), which is always greater than or equal to zero. For materials that manifest negligible strain rate sensitivity, m is near zero, making σ a constant. (Sapphire is an example of such a material.) Materials with greater strain rate sensitivity have greater values of m.

Provided that hardness (H) is directly related to plastic stress, then hardness also manifests this same phenomenon, giving the relation:

$$H = B\, \dot{\varepsilon}^m \quad \text{Eq. 2}$$

In Equation 2, B is a constant (though different in value from B* in Equation 1) and $\dot{\varepsilon}$ is the indentation strain rate, defined as the loading rate divided by the load ($\dot{P}/P$).[1] The strain rate sensitivity, m, has the same meaning and value in Equation 2 as it does in Equation 1. Taking the logarithm of both sides of Equation 2 and simplifying yields:

$$\ln(H) = m \cdot \ln(\dot{\varepsilon}) + \ln(B) \quad \text{Eq. 3}$$

Thus, for many materials, there is a linear relationship between the logarithm of hardness and the logarithm of strain rate, with the slope being the strain rate sensitivity, m.

So, in order to determine strain rate sensitivity, we must measure hardness over a range of strain rates. However, thermal drift—the natural expansion and contraction of the equipment and sample due to changing temperature—adversely affects hardness measurements at small strain rates, because such measurements take a long time. To illustrate the problem, let us say that we wish to measure the hardness of nickel at a strain rate of $\dot{\varepsilon}$ = 0.002/sec at a penetration depth of 250nm. At this strain rate, it takes about 1200 seconds (20 minutes) to reach a penetration depth of 250nm. Even if the thermal drift rate is limited to 1Å per second, this means that the displacement due to thermal drift may be as high as 120nm or 50% of the target displacement. Furthermore, there is no way to measure thermal drift by simply holding the force constant and measuring displacement, because the materials creep. Thus, any experimental procedure for measuring hardness at low strain rates must carefully consider and deal with the problem of thermal drift.

For many metals, elastic modulus is independent of strain rate. This has been demonstrated experimentally for nickel.[3,5] If this is true, then elastic modulus can be measured at a high strain rate (using an established test method) and then contact areas can be calculated for other strain rates as a function of measured elastic stiffness and known elastic modulus, thus bypassing the direct measurement of displacement altogether. This is the approach taken in the present work.[1]

Strictly, the term 'indentation strain rate' refers to the displacement rate divided by the displacement ($\dot{h}/h$). However, beginning with the definition of hardness, it is easily shown that $\dot{h}/h \approx 0.5(\dot{P}/P)$. Equation 2 holds true for either definition of strain rate, because the constant (0.5) difference between the two definitions is simply absorbed into the constant B. Because it is logistically easier to control $\dot{P}/P$ than $\dot{h}/h$, the term 'strain rate' refers to $\dot{P}/P$, unless specifically stated otherwise.

If the elastic modulus of the test material (E) is known, then contact area (A) can be calculated directly from the measured stiffness (S). We begin with Sneddon's stiffness equation[6] as commonly expressed for interpreting indentation data:[7, 8]

$$E_r = \frac{\sqrt{\pi}}{2}\frac{S}{\sqrt{A}}, \quad \text{Eq. 4}$$

where Er is the reduced elastic modulus, obtained from the elastic modulus and Poisson's ratio of the sample and indenter as

$$\frac{1}{E_r} = \frac{1-v^2}{E} + \frac{1-v_i^2}{E_i} \quad \text{Eq. 5}$$

Rearranging Equation 4 to solve for A yields:

$$A_E = \frac{\pi}{4}\frac{S^2}{E_r^2}\ . \quad \text{Eq. 6}$$

We use the notation A_E to represent area to convey the fact that area is calculated as a function of modulus. Hardness is calculated as the load divided by the contact area:

$$H_E = P/A_E\ . \quad \text{Eq. 7}$$

Furthermore, the area as calculated by Equation 6 can be used to determine displacements by inverting the area function.[1] This is straightforward, so long as the area function is a two-term function of contact depth, h_c. If the area function has the form $A = m_0 h_c^2 + m_1 h_c$, then the contact depth is given by:

$$h_{c-E} = \frac{-m_1 + \sqrt{m_1^2 - 4m_0 A_E}}{2m_0}. \quad \text{Eq. 8}$$

Finally, displacement is calculated as:

$$h_E = h_{C-E} + 0.75\ P/S, \quad \text{Eq. 9}$$

where P is the indentation force.

To summarize, at small strain rates thermal drift obfuscates the direct measurement of displacement from which contact area is normally calculated, so we calculate contact area indirectly as a function of modulus and stiffness (Equation 6). This is valid so long as the modulus is independent of strain rate. Both hardness and displacement are calculated using this indirect determination of contact area. In order to distinguish these parameters as being obtained as a function of modulus, we use A_E, H_E, and h_E to identify the area, hardness, and displacement obtained in this way.

Procedure

Samples. Four samples were tested in this work: fused silica, sapphire, a copper film on silicon and a nickel film on silicon. The first two samples were tested to provide an evaluation of the method. The two metallic films exemplify the kinds of samples for which this method ought to be used. Copper and nickel films were deposited on Si substrates by DC magnetron sputtering at room temperature. The base pressure of the chamber was 6×10-6Pa. Both copper and nickel films exhibited highly (111) texture. High density nanoscale twin structure with average spacing of ~20nm was observed only in the copper film.

Equipment. A KLA Nano Indenter® system with a Berkovich indenter tip was used for all testing. The Continuous Stiffness Measurement (CSM) option was also used in order to achieve hardness and elastic modulus as a continuous function of penetration depth.[9]

Test Method. This work required the use of two test methods—one established and one new. The established test method was first used to measure hardness and modulus of all four samples using common analysis.[9] (This test method does not employ the analysis described by Equations 6–9.) Twelve tests were performed on each sample to a depth limit of 500nm using a strain rate of 0.05/sec. For the fused silica and sapphire, properties were recorded at a penetration depth of 400nm. For the thin-film metals, properties were recorded at a penetration depth corresponding to 20% of the film thickness.

Next, the Accufilm method was used to evaluate hardness as a function of strain rate. This method automatically calculates contact area according to Equation 6, hardness according to Equation 7, contact depth according to Equation 8, and displacement according to Equation 9.[1] The modulus used for these calculations was the value obtained for the sample from the first set of measurements. On each sample, twelve indentation tests were performed at each of three different strain rates. The battery of 36 tests was executed twice on fused silica. For the fused silica and sapphire, H(E) was recorded for each test at a penetration depth of 400nm. For the thin-film metals, H(E) was recorded for each test at a penetration depth corresponding to 20% of the film thickness.

Results

The values of modulus are used to calculate area, hardness, and displacement according to Equations 6–9 in subsequent testing at slow strain rates.

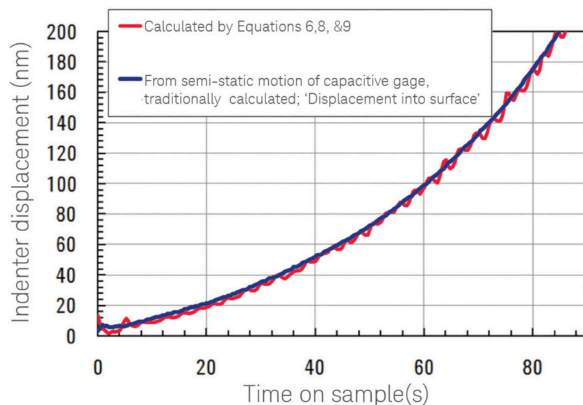

Figure 1. Displacement determined in two ways for a single indent on a nickel film tested at $\dot{\varepsilon}$ = 0.05/sec using the Accufilm method. The blue trace derives from regular analysis of the semi-static motion of the capacitive gauge. The red trace is calculated by assuming a constant modulus, the value of which was previously measured to be 224.1GPa by a common test method.

Figure 1 compares the two methods proposed in this work for determining displacement. Both traces in this plot derive from a single physical test on the nickel film using the Accufilm method at $\dot{\varepsilon}$ = 0.05/sec. The blue trace is obtained by applying common analysis to the output of the means for measuring displacement (a capacitive gauge). The red trace is obtained through Equations 6, 8, and 9 with the modulus set to 224GPa. Although the red trace is much "noisier," the two traces are very close throughout the test.

Figure 2 examines the same test as Figure 1, but compares the two ways of getting hardness. The blue trace is obtained by applying common analysis to the output of the means for measuring force, displacement, and stiffness. The red trace is obtained by applying Equations 6–9 with the modulus set to 224GPa. At this strain rate ($\dot{\varepsilon}$ = 0.05/sec), the blue trace is obviously superior, but the red trace carries the advantage of being impervious to thermal drift, which makes it ideal for low strain rate testing. Highlighted data around 20% of the film thickness were averaged to report a single value of hardness for this particular test.

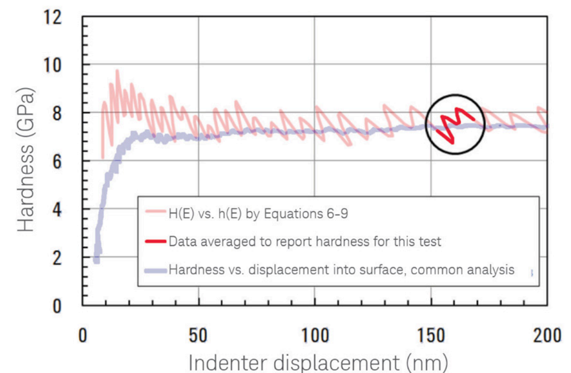

Figure 2. Hardness determined in two ways for a single indent on a nickel film tested at $\dot{\varepsilon}$ = 0.05/sec using the test method G-Series XP Thin Film SRS. msm. The blue trace derives from regular analysis of the CSM data. The red trace is calculated by assuming a constant modulus, the value of which was previously measured to be 224.1GPa by a common test method at h = 160nm (20% of tf). Highlighted data around 20% of the film thickness were averaged to report a single value of hardness for this test.

Figure 3 illustrates the advantage of the new analysis. This plot shows all twelve tests performed on nickel at $\dot{\varepsilon}$ = 0.01/sec using the Accufilm method. It should be noted that this strain rate is five times slower than the strain rate that is used for standard testing ($\dot{\varepsilon}$ =0.05/sec). The test-to-test variation in common hardness (blue) is entirely due to thermal drift. The new definition of hardness (red) is noisier, but more accurate.

Figures 4–7 show the results of the 36 tests on each sample in terms of ln(H(E)) vs. ln($\dot{\varepsilon}$). On these plots, one data point corresponds to one indentation test. For example, the highlighted data in Figure 2 were averaged to report a hardness of H(E)= 7.579GPa for one test on nickel at $\dot{\varepsilon}$ = 0.05/sec. This test appears plotted in red on Figure 7 at the position (ln($\dot{\varepsilon}$), ln(H(E))) = (-2.996, 2.025) The strain rate sensitivity is the slope of the best linear fit to each set of 36 points; the LINEST function in Microsoft® Excel® provides the standard error in this slope, which we take to be the uncertainty in the strain rate sensitivity.

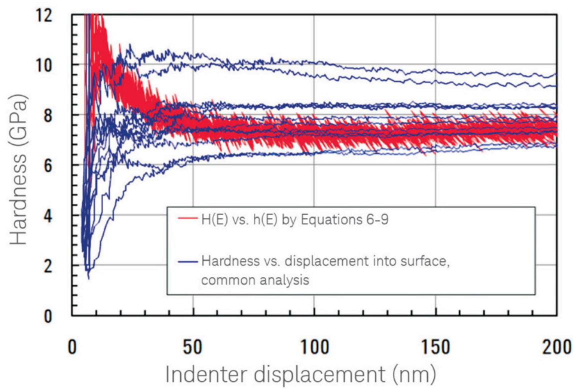

Figure 3. Hardness determined in two ways for all 12 tests on nickel film performed at $\dot{\varepsilon}$ = 0.01/sec using the the Accufilm method. Blue traces derive from common analysis of the CSM data; red traces derive from Equations 6–9 using a modulus of 224GPa. Though the red traces are "noisier," they are more accurate at small strain rates due to insensitivity to thermal drift.

Figure 4 shows the results for sapphire. The linear fit to these data yields a negative slope, m = –0.012 ±0.005. Although the slope value is obviously errant—the lower theoretical limit for m is zero—this is not unexpected, because sapphire has negligible strain rate sensitivity. If the value of a parameter is truly zero, then the experimental measurement of that parameter may very well be slightly negative. We are reassured by the fact that the magnitude of the measured value is comparable to the magnitude of the uncertainty.

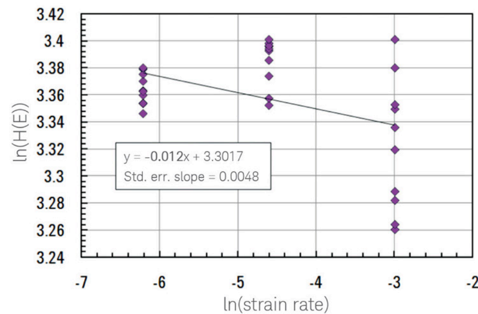

Figure 4. Ln(H(E)) vs. ln($\dot{\varepsilon}$) for twelve tests at each of three strain rates on sapphire. As expected, the procedure returns a near-zero strain rate sensitivity. The slope of the best linear fit is negative (m = -0.012); further, this magnitude is not much larger than the standard error (0.005).

Figure 5 shows the results of the two trials on fused silica (72 independent tests). Surprisingly, we found a significant, albeit small, strain rate sensitivity in this material. Figure 6 shows the results for the copper film, and Figure 7 shows the results for the nickel film.

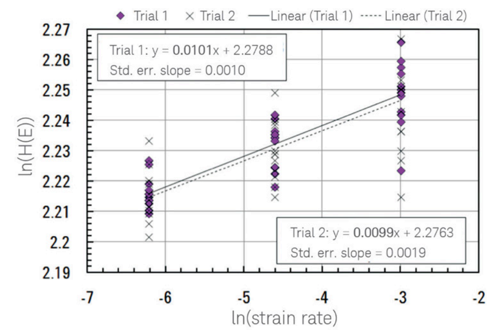

Figure 5. Ln(H(E)) vs. ln($\dot{\varepsilon}$) for two trials on fused silica, each of which comprised twelve tests at each of three strain rates. Surprisingly, the procedure returns a measurable value of strain rate sensitivity of fused silica; Trial 1: m = 0.0101 ±0.0010; Trial 2: m = 0.0099 ±0.0019.

The strain rate sensitivities obtained for the copper and nickel films meet expectations for these materials.

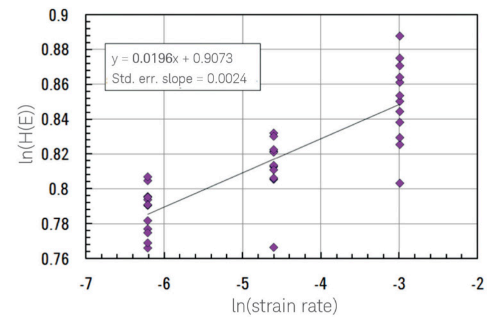

Figure 6. Ln(H(E)) vs. ln($\dot{\varepsilon}$) for twelve tests at each of three strain rates on (111) Cu film (t = 1500nm). The strain rate sensitivity is reasonable for copper; m = 0.0196 ±0.0024.

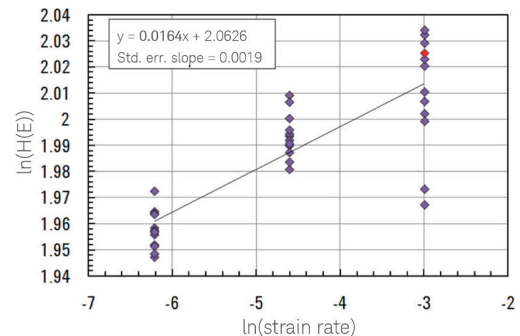

Figure 7. Ln(H(E)) vs. ln($\dot{\varepsilon}$) for twelve tests at each of three strain rates on (111) Ni film (t = 800nm). The strain rate sensitivity is reasonable for nickel; m = 0.0164 ±0.0019. The red point represents the highlighted data from Figure 2.

Discussion

This method for determining the strain rate sensitivity of thin films and other small volumes of material relies on knowing the elastic modulus of the material. However, the values of elastic modulus returned by the established method are high for the nickel and copper films. For nickel, the measured modulus (224GPa) is higher than the nominal modulus (200GPa) by about 12%. For copper, the measured modulus (153GPa) is higher than the nominal modulus (110-130GPa) by at least 18%. What causes these errors and to what extent do they affect the determination of strain rate sensitivity? The measured moduli of copper and nickel are high due to causes which are well understood.

The measured modulus of nickel is high due to 'pile-up.' When pile-up occurs, the model that is used to calculate contact area under-predicts the true contact area, and thus over-predicts the modulus, which is inversely related to the square root of contact area. The measured modulus of copper is high due to pile-up AND substrate influence, both of which tend to push the measured value higher with increasing indenter penetration. Established practices exist for addressing both pile-up and substrate influence. For example, measurements could be made at shallower depths, or an analytic model could be used to correct for substrate influence.[10] However, we assert that such measures are neither ideal nor necessary.

Substrate influence implies that the substrate has a measurable influence on the stiffness sensed by the indenter. If the ultimate goal is to calculate contact area as a function of stiffness and modulus by Equation 6, then the modulus that ought to be used in Equation 6 is that which corresponds to the measured stiffness at the displacement of interest—i.e., the substrate-affected value. But it turns out that the determination of strain rate sensitivity is not very sensitive to modulus, because what is important is the change in hardness due to change in strain rate, not the absolute value of hardness. To verify this, we may calculate the strain rate sensitivity for the copper and nickel films using moduli values of 130GPa and 200GPa, respectively. The resulting strain rate sensitivity of the copper film comes out to 0.0192 ±0.0019 and the strain rate sensitivity of the nickel film comes out to 0.0188 ±0.0016. The precise value of modulus has very little influence on the strain rate sensitivity achieved by this method.

At least one indentation manufacturer offers a dual-probe design in order to deal with the problem of thermal drift. The principle of operation is that a reference probe rests on the surface in order to follow the thermal expansion/contraction of sample and equipment, while a second probe performs the indentation test. The relative difference in displacement between the indentation probe and the reference probe is taken to be the true displacement. However, this approach is futile if the material creeps in response to the force of the reference probe, because the difference between the two probe positions then excludes the very response that one wishes to examine—time-dependent deformation. The only materials for which long testing times are interesting are the very materials that will creep in response to a reference probe. Thus, the reference probe design fails as a solution for the problem of thermal drift under precisely those circumstances in which a solution is most needed—that is, when monitoring the deformation of elastic materials over long periods of time.

The dynamic measurement of stiffness by means of the CSM option is an essential aspect of this procedure for two reasons. First, accurate knowledge of the elastic modulus is prior to and essential to this procedure. For metals that manifest substantial creep, the contact stiffness (S) cannot be obtained accurately from the slope of the unloading curve, because the unloading curve manifests both elastic recovery and creep; there is no practical way to deconvolute one from the other. For such materials, the stiffness—and thus the elastic modulus—can only be measured accurately by means of the small oscillation used by the CSM option. Second, once the elastic modulus is known, CSM is used to accurately determine hardness values that are insensitive to thermal drift, even for very low-strain rate indentations.

Conclusion

The Student's t-test is used in an uncommon way to predict the number of observations (N) which must be made in order to be sensitive to a given difference at a given confidence level. Subject to a few simplifications, N depends on three things: the difference in means one wishes to sense (F), the normalized variance (q2), and the desired confidence level. This analysis is appropriate for any kind of experimentation to which the Student's t-test might apply. With respect to nanoindentation, this analysis illuminates the benefits of the ultra-fast testing afforded by the Express Test or NanoBlitz 3D options for the KLA Nano Indenter® systems. Because it allows many more independent observations in a given time frame, Express Test or NanoBlitz 3D dramatically improves sensitivity to significant difference.

KLA

References

1. Weihs, T.P. and Pethica, J.B., Monitoring time-dependent deformation in small volumes, Mater. Res. Soc. Symp. Proc. 239, 325-330, 1992.

2. Maier, V., Merle, B., Goeken, M., and Durst, K., An improved long-term nanoindentation creep testing approach studying the local deformation processes in nanocrystalline metals at room and elevated temperatures, Journal of Materials Research 28(9), 1177-1188 2013.

3. Maier, V., Durst, K., Mueller, J., Backes, B., Hoppel, H., and Goeken, M., Nanoindentation strain rate jump tests for determining the local strain rate sensitivity in nanocrystalline Ni and ultrafine-grained Al, Journal of Materials Research 26(11), 1421-1430, 2011.

4. Ye, J.C., Wang, Y.M., Barbee, T.W., and Hamza, A.V., Orientation-dependent hardness and strain rate sensitivity in nanotwin copper, Applied Physics Letters 100(261912), 1-6, 2012.

5. Hay, J.L., Maier, V., Durst, K., and Goeken, M., Strain Rate Sensitivity (SRS) of Nickel by Instrumented Indentation, Keysight Technologies, Inc., 2011, Document No: 5990-9434EN.

6. Sneddon, I.N., The Relation Between Load and Penetration in the Axisymmetric Boussinesq Problem for a Punch of Arbitrary Profile, Int. J. Eng. Sci. 3(1), 47-57, 1965.

7. Oliver, W.C. and Pharr, G.M., An Improved Technique for Determining Hardness and Elastic-Modulus Using Load and Displacement Sensing Indentation Experiments, Journal of Materials Research 7(6), 1564-1583, 1992.

8. Pharr, G.M., Oliver, W.C., and Brotzen, F.R., On the Generality of the Relationship among Contact Stiffness, Contact Area, and Elastic-Modulus during Indentation, Journal of Materials Research 7(3), 613-617, 1992.

9. Hay, J.L., Agee, P., and Herbert, E.G., Continuous Stiffness Measurement during Instrumented Indentation Testing, Experimental Techniques 34(3), 86-94, 2010.

10. Hay, J.L. and Crawford, B., Measuring Substrate-Independent Modulus of Thin Films, Journal of Materials Research 26(6), 2011.

This application note was created by Yue Liu and Xinghang Zhang, Department of Mechanical Engineering, Texas A&M University, College Station, TX, United States.

Microsoft and Excel are registered trademarks of Microsoft Corporation.

KLA SUPPORT
Maintaining system productivity is an integral part of KLA's yield optimization solution. Efforts in this area include system maintenance, global supply chain management, cost reduction and obsolescence mitigation, system relocation, performance and productivity enhancements, and certified tool resale.

© 2019 KLA Corporation. All brands or product names may be trademarks of their respective companies. KLA reserves the right to change the hardware and/or software specifications without notice.

KLA Corporation
One Technology Drive
Milpitas, CA 95035
www.kla.com

Printed in the USA
2019-01